Journal of the Atmospheric Sciences (submitted)

A Mechanism and Simple Dynamical Model of the North Atlantic Oscillation and Annular Modes

GEOFFREY K. VALLIS, EDWIN GERBER,
PAUL J. KUSHNER AND BENJAMIN A. CASH
GFDL, Princeton University

(27 February 2003)

ABSTRACT

We present a simple dynamical model for the basic spatial and temporal structure of the large-scale modes of intraseasonal variability and associated variations in the zonal index. Such variability in the extra-tropical atmosphere is known to be represented by fairly well-defined patterns or modes, and among the most prominent are the North Atlantic Oscillation (NAO) and a more zonally symmetric pattern known as an annular mode, which is most pronounced in the Southern Hemisphere. We suggest that these patterns are a direct consequence of the stirring effects of baroclinic eddies, and we explicitly show how such stirring, as represented by a simple random forcing in a barotropic model, leads to a variability in the zonal flow via a variability in the eddy momentum flux convergence and to patterns similar to those observed. Typically, the leading modes of variability may be characterized as a mixture of 'wobbles' in the zonal jet position and 'pulses' in the zonal jet strength. If the stochastic forcing is statistically zonally uniform, then the resulting patterns of variability (i.e., the empirical orthogonal functions) are zonally uniform and the pressure pattern is dipolar in the meridional direction, resembling an annular mode. If the forcing is enhanced in a zonally localized region, thus mimicking the effects of a stormtrack over the ocean, then the resulting variability pattern is zonally localized, with a pattern resembling the North Atlantic Oscillation. This suggests that the North Atlantic Oscillation and annular modes are produced by the same mechanism, and are manifestations of the same phenomenon.

The timescale of variability of the patterns is longer than the decorrelation timescale of the stochastic forcing, being reddened by nonlinear dynamics and by the linear effects of friction. For reasonable parameters this produces a decorrelation time of order 10 days. The model also produces some long term (e.g., 100–1000 days) variability, without imposing such variability via the external parameters except in the nearly white stochastic forcing.

1. Introduction

The large-scale atmospheric circulation displays variability on multiple timescales. The most prominent variability in the extratropics is that due to baroclinic eddies, or midlatitude weather systems, which typically have a timescale of a few days. On timescales of a season or longer atmospheric variability may be influenced by interactions at its boundaries (e.g., by the sea-surface temperature) and by other slow changes in forcing. The variability on intermediate (i.e., intraseasonal) timescales, say between 10 days and a season (and often confusingly called 'low-frequency' variability) has a less obvious cause. The direct effect of the ocean or other changing boundary seems unlikely to be important, both because large-scale sea-surface temperatures tend to change primarily on still longer timescales and because their effect is unlikely to be strong enough to produce discernible changes in the atmospheric circulation on the 10–100 day timescale. Rather, we expect that this variability has a primarily atmospheric origin, ultimately arising from baroclinic activity and weather systems and reddened by frictional or nonlinear processes. The dynamics of such variability, however, is not fully understood, and is the subject of this paper.

Although we may refer to intraseasonal variability as if there were a distinct timescale and a distinct phenomenon, there is no pronounced peak in the power spectrum of the atmospheric fields on the weeks-to-months timescale, but nor is there a dip in the spectrum at timescales longer than that associated with baroclinic eddies. This suggests that the variability at intraseasonal timescales may be, at leading order, caused by a reddening of the power spectrum of the known forcing (i.e., baroclinic instability) by frictional processes and/or the nonlinear dynamical effect of a cascade of variance to larger spatial scales and longer frequencies. At still longer timescales, there may be additional power on the year-to-decade timescale, and whether this can have a purely atmospheric origin is not known.

If the atmospheric fields are appropriately filtered in time to select intraseasonal timescales, then fairly well-defined spatial patterns of variability emerge. This spatial structure has been the object of much study and debate, going back at least as far as Walker and Bliss (1932), and summarized recently by Wallace (2000) and Wanner et al. (2002). The patterns robustly show up in correlation maps or teleconnection patterns (Wallace and Gutzler 1981), and in the Empirical Orthogonal Functions (EOF) of the low-passed fields (e.g., Ambaum et al. 2001), and a host of such patterns have been identified by these and other workers – the North Atlantic Oscillation (NAO), the Northern and Southern Annular Modes (NAM, SAM), the Pacific North American pattern (PNA), the Pacific Decadal Oscillation (PDO) and so on. Of these the North Atlantic Oscillation is probably the most well known and this, and the annular modes (Thompson and Wallace 2000), will mainly concern us in this paper. The scale of these patterns is significantly larger than that typically associated with a single baroclinic eddy, ranging from a few thousand kilometers of the NAO to the hemispheric scale of the annular modes. Two other aspects of their structure stand out: (i) They are barotropic, or at least equivalent barotropic (little phase shift in the vertical); (ii) There is a strong dipolar component in the horizontal structure of the pressure field.

Although the patterns are of larger scale than baroclinic eddies, there is much to suggest that such eddy activity (i.e., weather systems) is largely responsible for producing them, even though the patterns are fairly barotropic. On the theoretical side, large-scale eddy-driven structures often tend to be barotropic because the life-cycle of baroclinic eddies is characterized by a barotropic decay and a cascade to larger horizontal *and vertical* scales (Rhines 1977; Simmons and Hoskins 1978; Salmon 1980), and idealized model simulations (e.g., Orlanski 1998) have shown the important role of baroclinic eddies in producing the quasi-stationary circulation. On the observational side, analysis of annular modes and the NAO indicates that transient, high frequency (i.e., 1–10 days) activity plays an important role in maintaining their variability (e.g., Lau 1988; Limpasuvan and Hartmann 2000; DeWeaver and Nigam 2000). Consistently, the midlatitude jet in the Atlantic sector is stronger during periods of high NAO index [Ambaum et al. (2001), their figures 6 and 7], and this jet is fairly barotropic, indicating an eddy-driven origin. Finally, recent experiments with a GCM (Cash et al. 2002) have shown a strong correlation between the location and strength of the dipole with the location and strength of the baroclinic eddy activity.

Assuming, then, that the relevant large-scale dynamics are indeed barotropic, but that that eddy activity is important as the ultimate source of the variability, our goal now is to understand how such higher-frequency (1–10 day timescale) eddy dynamics can produce the characteristic spatial patterns seen on longer (10–100 day) timescales. Specifically, we seek to present a simple dynamical model, perhaps the simplest possible dynamical model, of the NAO and annular modes in order to shed insight on the dynamics of such structures. We shall not present a complete model or a complete theory. Rather, our model might be considered as a 'dynamical null-hypothesis' that might be built upon to create a more complete theory.

2. The Basic Model

a. Jets on a β-plane

Consider first the maintenance of the extratropical jet. This has a different dynamical origin from the highly baroclinic subtropical jet: the latter arises from a thermal wind balance with the strong meridional temperature gradients at the edge of the Hadley Cell, whereas the former is driven by eddy momentum flux convergence in midlatitude weather systems and, because these largely occur in the mature phase of the baroclinic lifecycle, they act to produce a predominantly barotropic jet. In reality the subtropical and midlatitude jet are often not geographically distinct because the polar limit of the Hadley cell overlaps the equatorial limit of the midlatitude baroclinic zone, and the jets may appear as one.

A simple barotropic model illustrates the mechanisms of the eddy driven jet (e.g., Held 2000). For two-dimensional incompressible flow the barotropic zonal momentum equation is

$$\frac{\partial u}{\partial t} + u\frac{\partial u}{\partial x} + v\frac{\partial u}{\partial y} - fv = -\frac{\partial \phi}{\partial x} + F_u - D_u \quad (2.1)$$

where F_u and D_u represent the effects of any forcing and dissipation and the other notation is standard. The meridional momentum and vorticity fluxes are related by the identity

$$v\zeta = \tfrac{1}{2}\frac{\partial}{\partial x}\left(v^2 - u^2\right) - \frac{\partial}{\partial y}(uv) \quad (2.2)$$

so that with cyclic boundary conditions

$$\overline{v'\zeta'} = -\frac{\partial \overline{u'v'}}{\partial y}. \quad (2.3)$$

where the overbar denotes a zonal average, and $\overline{v} = 0$. Equation (2.3) also holds, locally in x, if the average is a time or ensemble average provided that the eddy statistics are zonally uniform. Averaging (2.1) thus gives

$$\frac{\partial \overline{u}}{\partial t} = \overline{v'\zeta'} + \overline{F}_u - \overline{D}_u \tag{2.4}$$

again using that $\overline{v} = 0$, a result that again also holds in a time or ensemble average if the eddy statistics are zonally uniform.

Typically, there will be little direct forcing of the mean momentum, and if friction is parameterized by a linear drag then

$$\frac{\partial \overline{u}}{\partial t} = \overline{v'\zeta'} - r\overline{u} \tag{2.5}$$

where r is an inverse frictional timescale. Now consider the maintenance of this vorticity flux. The barotropic vorticity equation is

$$\frac{\partial \zeta}{\partial t} + \boldsymbol{u} \cdot \nabla \zeta + v\beta = F_\zeta - D_\zeta \tag{2.6}$$

where F_ζ parameterizes the stirring of barotropic vorticity and D_ζ represents dissipation. Linearize about a mean zonal flow to give

$$\frac{\partial \zeta'}{\partial t} + \overline{u}\frac{\partial \zeta'}{\partial x} + \gamma v = F'_\zeta - D'_\zeta \tag{2.7}$$

where

$$\gamma = \beta - \frac{\partial^2 \overline{u}}{\partial y^2} \tag{2.8}$$

is the meridional gradient of absolute vorticity. From (2.7) form the pseudo-momentum equation by multiplying by ζ'/γ and zonally averaging, whence

$$\frac{\partial M}{\partial t} - \overline{v'\zeta'} = -\frac{1}{\gamma}(\overline{\zeta' F'_\zeta} - \overline{\zeta' D'_\zeta}) \tag{2.9}$$

where

$$M = -\frac{1}{2\gamma}\overline{\zeta'^2} \tag{2.10}$$

is the pseudomomentum. From (2.5) and (2.9) we obtain

$$\frac{\partial \overline{u}}{\partial t} - \frac{\partial M}{\partial t} = -r\overline{u} + \frac{1}{\gamma}(\overline{\zeta' F'_\zeta} - \overline{\zeta' D'_\zeta}), \tag{2.11}$$

and in a statistically steady state

$$r\overline{u} = \frac{1}{\gamma}(\overline{\zeta' F'_\zeta} - \overline{\zeta' D'_\zeta}). \tag{2.12}$$

As the terms on the right-hand-side represent the stirring and dissipation of vorticity, then meridionally localised but otherwise relatively unstructured vorticity stirring will give rise (for $\gamma > 0$) to an eastward mean zonal flow in the region of the stirring, with a westward flow north and south of the stirring region. These equations represent the well-known physical argument that stirring gives rise to Rossby wave generation, and that momentum will converge in the region of stirring as the Rossby waves propagate away and dissipate.

If the stirred region is sufficiently broad then multiple jets may form within the stirring region (e.g., Vallis and Maltrud 1993; Lee 1997). In that case the mechanism of jet formation is then often expressed in terms of an inverse energy cascade to larger scales, inhibited by the formation of Rossby waves, leading to the preferential formation of zonal flow. However, such jets may still be considered to be maintained by the stirring of pseudomomentum, but the pseudomomentum stirring, $(\overline{\zeta' F'_\zeta})/\gamma$, is organized by the jet structure itself even though the vorticity stirring, F_ζ, may be homogeneous. In the earth's atmosphere the stirring region (i.e., the midlatitude baroclinic zone) is relatively narrow in the sense that there is normally only one region of eddy driven eastward flow in the mean; however, the baroclinic zone is typically wider than the instantaneous jet itself, and the jet may thus meander within the baroclinic zone.

b. Source of stirring in a baroclinic atmosphere

The stirring that might generate such jets arises from baroclinic instability or, more precisely, from the transfer of energy from baroclinic to barotropic modes. To see this, consider the two-layer quasi-geostrophic equations

$$\frac{\partial q_i}{\partial t} + J(\psi_i, q_i) = 0, \qquad i = 1, 2 \tag{2.13}$$

where

$$q_i = \nabla^2 \psi_i + F(\psi_j - \psi_i) + \beta y, \qquad j = 3 - i. \tag{2.14}$$

and F is the inverse square deformation radius. If this is decomposed into barotropic and baroclinic modes in the standard way, the evolution equation for the barotropic mode becomes

$$\frac{\partial}{\partial t}\nabla^2 \psi + J(\psi, \nabla^2 \psi + \beta y) = J(\tau, \nabla^2 \tau) \tag{2.15}$$

where $\psi = (\psi_1 + \psi_2)/2$ and $\tau = (\psi_1 - \psi_2)/2$. The term on the right-hand-side is just the stirring of the

barotropic mode by the baroclinic mode, leading to transfer of energy into the barotropic mode as part of the baroclinic lifecycle. Such stirring by baroclinic eddies thus gives rise to momentum convergence and is the ultimate cause of the surface westerly winds in midlatitudes. The vorticity flux producing the zonal jet will, of course, fluctuate simply because baroclinic activity fluctuates, partly in response to variations in the zonal shear itself and partly because it is a turbulent, chaotic system, and these fluctuations will give rise to variations in the zonal index (e.g., Feldstein and Lee 1998; Lorenz and Hartmann 2001). Although such variations will be largely barotropic, the stirring will be dependent in part on the barotropic flow, because the evolution equation of τ involves ψ, and this may lead to feedbacks between the jets and the stirring. For example, the presence of surface drag may generate a shear from the barotropic flow, and this in turn may produce baroclinic activity and enhanced stirring (Robinson 2000). In our numerical simulations, we will restrict ourselves to the simpler barotropic case and will model the stirring simply by a random process with time and space scales chosen to roughly mimic those of baroclinic instability, with no direct dependence on the jet itself.

c. *Patterns of variability*

Because the stirring is produced by a chaotic process it will fluctuate, and this will produce a response in the zonal wind field and the associated circulation. In particular, a fluctuation in the vorticity flux that has a simple meridional structure will produces a dipolar structure in the pressure or streamfunction field. To illustrate this, Fig. 1 shows a localized northward eddy flux of vorticity (light arrows). Two circuits are shown as solid contours with circulation $\Gamma = \oint u_t \, ds$, where u_t is the velocity component tangential to the circuit. With the mechanical damping, we have

$$\frac{d\Gamma}{dt} = \oint u_n \zeta \, ds - r\Gamma \tag{2.16}$$

where u_n is the velocity component normal to the (right-hand oriented) circuit. Because the flow is incompressible, $\oint u_n \, ds = \oint (\partial\psi/\partial s) \, ds = 0$, where ψ is the streamfunction. Thus, if an overbar (e.g., $\overline{u}$) denotes the average along the circuit, and a prime (u') the departure from this average, then

$$\frac{\partial \overline{u}_t}{\partial t} = \overline{u'_n \zeta'} - r\overline{u_t}, \tag{2.17}$$

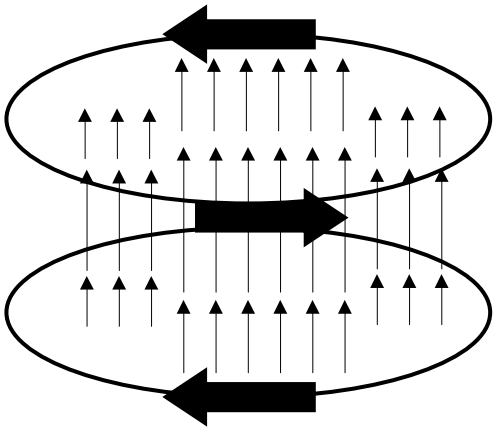

FIGURE 1: Circulation pattern induced by anomolous vorticity fluxes. The light arrows represent time- or ensemble-mean fluxes of eddy vorticity. The contours represent circuits for the calculation of circulation. The heavy arrows on the circuits represent the circulation that results from the eddy vorticity flux.

and for the time average in addition to the circuit average

$$\overline{u_t} = \overline{u'_n \zeta'}/r. \tag{2.18}$$

Thus, a time-mean eddy flux of vorticity out of the circuit will give rise to a mean circulation. In Fig. 1, to the north of the maximum vorticity flux, a cyclonic circulation will result, and to the south an anticyclonic circulation. This change in sign of the circulation corresponds to a change in sign of the streamfunction; if the pattern of vorticity flux is interpreted as an anomaly from a climatology, the eddy vorticity flux then produces a dipolar circulation anomaly. If the fluctuation is zonally symmetric, then the circulation anomaly will extend around the hemisphere. If the fluctuation is confined to some region of longitude as in Fig. 1, then the fluctuation will be a zonally localized dipole, rather like the NAO.

The argument above provides information about the circulation around a closed loop and, formally, says nothing about the zonal velocity itself. Of course the loop may extend around a latitude circle, in which case u_t is the zonal velocity and we recover (2.5). However, although (2.9) and (2.12) apply strictly only to the zonally averaged flow, we may also expect that locally stronger stirring will give rise to a locally stronger and more variable zonal jet. To see this, note that if the zonal scale over which the eddy statistics vary is longer than the meridional scale, then the first term on the right-hand-side of (2.2) will be smaller than the second term, after time averaging, and (2.3) will *approximately* hold. Similarly,

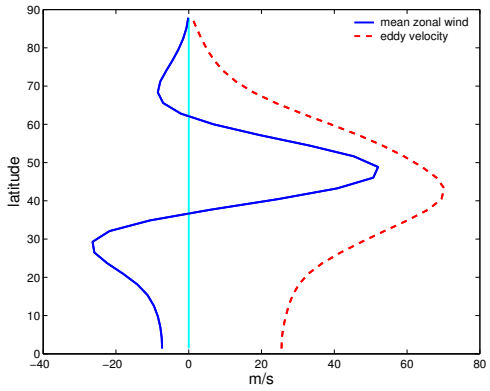

FIGURE 2: The time and zonally averaged zonal wind (solid line) from the zonally symmetric numerical model, Z1. The dashed line is the rms (i.e., eddy) velocity. The stochastic forcing is zonally uniform, centered at 45°.

the zonal advection of momentum in (2.1) will be smaller than that of meridional momentum, and the upshot is that (2.5) will approximately hold, with the overbar representing an average over a zonal sector without the need for complete zonal averaging.

Thus, in broad regions of enhanced stirring (e.g., the stormtrack regions) we expect to observe two related phenomena: (i) A stonger and more variable zonal jet; (ii) streamfunction or pressure anomalies that have the dipolar structure noted above. Furthermore, because these are anomaly fields, any diagnostic that seeks to economically represent the patterns of pressure or streamfunction variability, for example the EOFs, will also have a dipolar structure, and this is of course the characteristic pattern of the NAO. The latitude of the node of the mean streamfunction dipole will be that at which the mean vorticity flux is largest, and this is latitude of the mean jet itself. However, the distribution of the anomolous fluxes need not coincide with that of the mean fluxes, and we will see in section 4 that the node of the EOF of the streamfunction, representing the variability of the pattern, is often poleward of the jet and associated with a change in the position of the jet.

Finally, regarding the temporal structure of the response, suppose that, for simplicity, the stirring is white noise. Then, because of the effects of friction in (2.5), and possibly the inverse cascade, the response will be redder than the stirring – that is to say, it will have more power at lower frequencies. Thus, the posited patterns will be most apparent in the temporally low-passed fields, as this will filter the noise of the stirring itself.

3. Numerical model

To see whether eddy stirring can indeed produce the characteristic spatial patterns and temporal variability of annular modes and the NAO, we integrate the barotropic vorticity equation on the sphere, namely

$$\frac{\partial \zeta}{\partial t} + J(\psi, \zeta + f) = S - r\zeta + \kappa \nabla^4 \zeta. \qquad (3.1)$$

The notation is standard, with $f = 2\Omega \sin\vartheta$, where ϑ is latitude, ζ is vorticity and ψ streamfunction. The model is spectral with the nonlinear term evaluated without aliasing using a spectral transform method. Typically, the model is run at a resolution of T42 with test integrations at T84; this is more than adequate resolution because our concern is large-scale patterns. The last two terms on the right hand side of (3.1) are a linear drag and a term to remove the enstrophy that cascades to small scales, being the simplest parameterizations of those processes that remove momentum and enstrophy from the flow. The coefficient κ depends on the model resolution, for that term is a subgridscale closure. The linear drag has some physical grounding in Ekman layer theory, and for a barotropic representation of the atmosphere a reasonable value of r is of order $1/10\,\text{days}^{-1}$.

The term S represents stirring of the barotropic flow by baroclinic eddies, and we represent this by a Markov process, similar to that employed in Maltrud and Vallis (1991). Typically, we choose to excite a small range of wavenumbers, $n_{\min} < n < n_{\max}$ where n is the total wavenumber and, for example, $n_{\min} = 8$ and $n_{\max} = 12$, except that small zonal wavenumbers, including the zonal flow, are excluded from the forcing. Ideally, we would prefer not impose any particular timescale on the variability of the model fields, but a white noise forcing (which has equal amplitudes at all timescales) is not particularly realistic or appropriate, because the highest realizable frequencies would be timestep dependent and would not generate much response in the vorticity field, leading to a very noisy solution. Rather, we choose the random forcing to have a decorrelation timescale of about two days, similar to that of baroclinic instability. We satisfy this by making the forcing in each wavenumber, S_{mn} to be outcome of the stochastic process

$$\frac{dS_{mn}}{dt} = \dot{W}_{mn} - S_{mn}/\tau \qquad (3.2)$$

where $\dot{W}$ is a white noise process (a different realisation for each wavenumber) and the parameter τ determines the decorrelation time of the forcing. To

Experiment	Forcing Wavenumbers	Meridional half-width of stirring region	Zonally symmetric
Z1	11 – 13	12°	Yes
Z2	7 – 9	12°	Yes
A1	11 – 13†	12°	No (single enhanced region)
A2	11 – 13†	12°	No (two enhanced regions)

TABLE 1: Parameters for numerical experiments. Experiments with varying parameters are branches off $Z1$, unless noted. The decorrelation timescale of the forcing is always 2 days. († In the asymmetric cases the forcing wavenumbers are modified because the forcing is zonally asymmetric, which introduces an additional low wavenumber forcing.) The damping timescale is 10^6 s, or approximately 12 days, for all experiments illustrated, except as in Figs. 16 and 17. The stirring region has a Gaussian distribution in latitude, $\exp[(\vartheta - \vartheta_0)^2/2\sigma_\vartheta^2]$, and the 'half-width' is actually the standard deviation, σ_ϑ, of this. The zonally asymmetric forcing for A1 is described by (5.1), with $B = 1$.

implement (3.2), we use the related finite difference equation (see Appendix),

$$S^i_{mn} = \left(1 - e^{-2dt/\tau}\right)^{1/2} Q^i + e^{-dt/\tau} S^{i-1}_{mn} \qquad (3.3)$$

where Q^i is chosen randomly and uniformly $\in (-A, A)$ where A determines the overall forcing amplitude, dt is the model timestep, the superscript i is the timestep index, and τ is the prescribed decorrelation time of the forcing, which we typically choose to be two days. This spectral forcing is then transformed to physical space, where it is masked such that it has a non-negligible amplitude only in midlatitudes, typically between about 40° and 60° latitude. For some experiments it is also made statistically zonally nonuniform; that is, it is enhanced in a region about 45° wide in longitude, to mimic the effects of enhanced stirring in stormtracks. Instantaneously, the forcing is zonally nonuniform, and in all cases is constructed to have zero projection on the zonally symmetric flow (i.e., all components with $m = 0$ are zero at all times).

Apart from this meridional masking and the choice of the scale of the stirring, the stochastic forcing is relatively unstructured, and the resulting momentum flux convergences result from the nonlinear dynamics of the model. This type of stochastic model differs from that used in, for example, Branstator (1992) or Whitaker and Sardeshmukh (1998), in which the model is linear and the mean flow is taken from observations or a GCM. Here the model is nonlinear, and it is the stochastic forcing in conjunction with nonlinear dynamics that generates the mean flow, and that is important for its pattern of variability.

4. Spatial Structure of Model Variability

a. Mean state for zonally symmetric model

A typical time and zonally averaged zonal wind, and the rms (i.e., eddy) velocity are illustrated in Fig. 2. The stochastic forcing is a Gaussian centered at 45° with a standard deviation of 12°, and a decorrelation timescale of two days. A strong westward jet emerges in the region of the forcing, flanked by two eastward jets, rather stronger on the equatorial side indicating enhanced wave breaking on that side. Consistently, the mean position of the jet is somewhat poleward of the center of the stirring, and this polewards offset increases slightly as the forcing strength increases. The eddy velocities are of the same magnitude, albeit a little larger than, the zonally averaged velocity, a characteristic also of the flow in the earth's atmosphere. This is a consequence of the rather limited inverse cascade, in both model and atmosphere, which limits the magnitude of the eddies.

The natural meridional scale of a jet in homogeneous barotropic turbulence is determined by the eddy kinetic energy, and the value of β and friction (e.g., Smith et al. 2002). As noted above, if the meridional extent of the forcing region is allowed to become larger than that jet scale, multiple jets may form within the forcing region. This phenomena is illustrated in Fig. 3. Interestingly, the transitions from one jet regime to another are not smooth; for example, as the forcing region broadens sufficiently there is a sharp transition from one jet to two, and the locations of the ensuing two jets are both quite different from that of the single jet.

b. Variability

Now consider the variability of a single, eddy-driven zonal jet. Consider the momentum equation (2.5) and suppose that the vorticity flux is such as to pro-

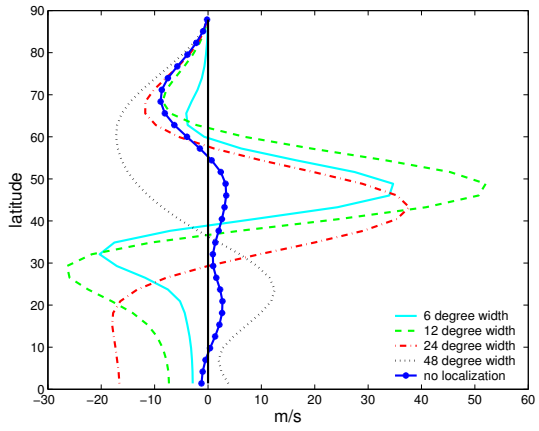

FIGURE 3: Time and zonally averaged zonal flow in experiments with varying widths (standard deviations) of the forcing zone, but otherwise the same forcing as Z1. If the forcing zone is narrow, then a single eastward jet forms in the region of the forcing. For a wide enough forcing zone, alternating jets can form within the forcing zone.

duce an eastward jet in midlatitudes, and that its magnitude fluctuates temporally but that its meridional structure remains fixed. Then the zonally averaged zonal wind will fluctuate in place – it will pulse – and the associated EOF of the zonal wind will be similar to that of the mean wind (Fig. 4a). Since at each instant the pressure field (the streamfunction) and the velocity are linearly related the associated variability in the pressure field can be expected to be a dipole. If the zonal wind fluctuates in this way, the node of the pressure EOF will coincide with the maximum of the jet, which in turn occurs where the stirring is strongest.

The other dominant mode of variability might be termed a wobbling of the zonal jet, that is an oscillation in its latitude without necessarily any change in amplitude (Fig. 4b). Both pulsing and wobbling behaviour frequently occur in numerical simulations, and one factor determining which is dominant is the width of the stirring region (Fig. 5). If the stirring region is wider than the natural width of a single jet, but not sufficiently wide to support two jets, the jet's position can vary within the stirred region, whereas if the stirring region is very narrow the jet position is effectively fixed (Fig. 5). The meridional structure of a pure pulsing EOF more-or-less mirrors that of the jet itself with a tripolar structure in the zonal wind, and the wobbling mode is in quadrature with this.

With a stirring region of similar meridional extent to that of the baroclinic zone on earth a wobbling or a 'mixed' mode tends to prevail (Fig. 6). Typically

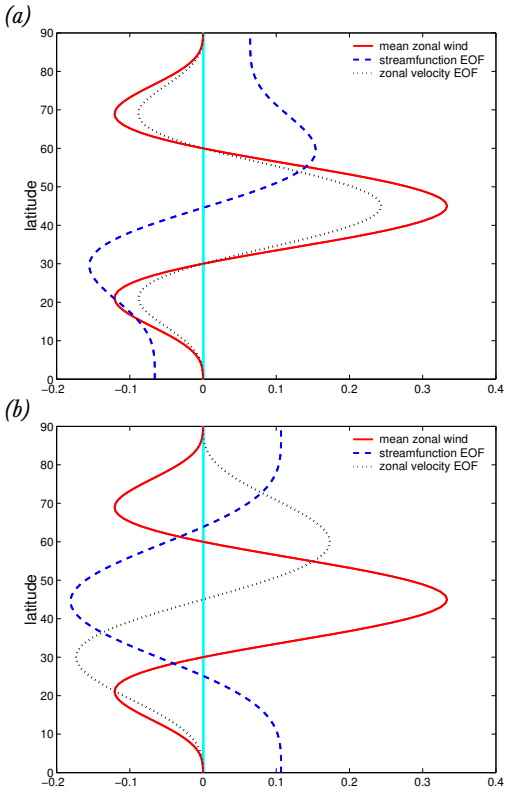

FIGURE 4: (a) Schematic of the leading EOF associated with a pulsing jet. Solid line is the mean zonal wind itself, the dotted line is the EOF of the zonal velocity and the dashed line the EOF of the pressure or streamfunction field. (b) As for (a) but for the leading EOF associated with a wobbling or oscillating jet.

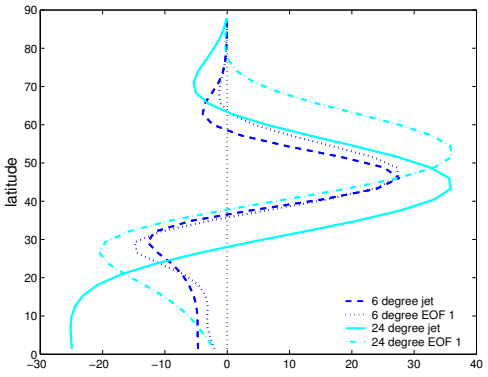

FIGURE 5: Mean jets and first EOFs for simulations with a narrow stirring region (approximately 6° half-width) and a broader stirring region (approximately 24° half-width), but otherwise the same forcing as Z1. In the former case the first EOF is a pulse, and resembles the jet itself. In the latter case the first EOF is a wobble, almost in quadrature with the jet.

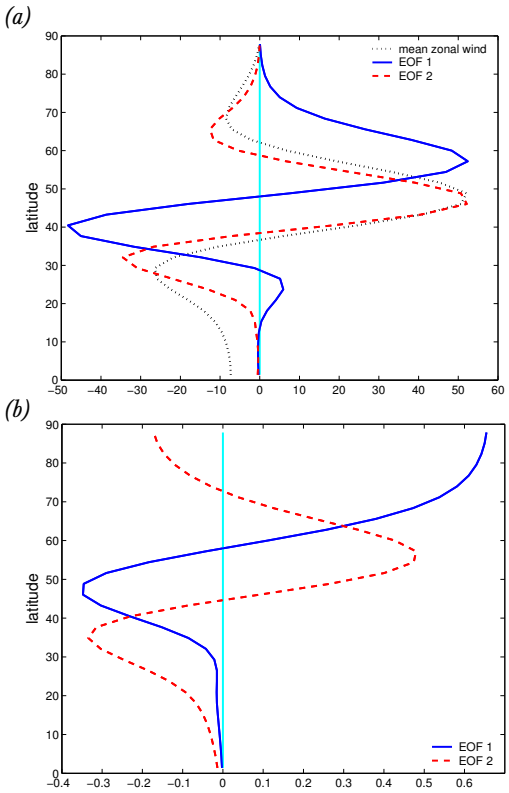

FIGURE 6: (a) The first two EOFs (solid and dashed, respectively) of the zonally averaged zonal wind corresponding of the model Z1. The solid line corresponds to a 'wobbling' zonal wind, the dashed to a 'pulsing' zonal wind. The light dotted line is the mean zonal wind. (b) Corresponding EOFs of the zonally averaged streamfunction.

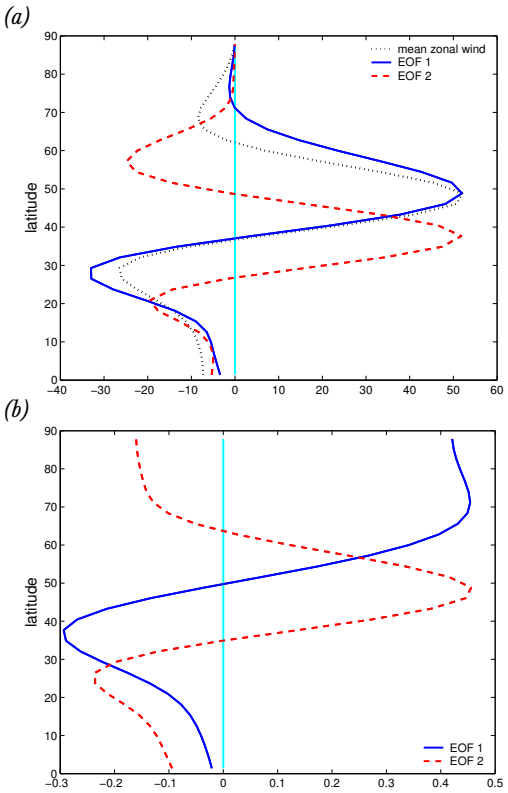

FIGURE 7: (a) The first two EOFs (solid and dashed, respectively) of the zonally averaged zonal wind corresponding to the solution of Z2. The EOFs are combinations of pulses and wobbles. (b) Corresponding EOFs of the zonally averaged streamfunction.

we find that the wobbling EOF is dominant when the zonal scale of the stochastic forcing is around wavenumber 10 or of smaller scale (higher wavenumber). For a larger scale forcing, the first EOF tends to be a mix of wobbling and pulsing modes of variability, as in Fig. 7; rarely is the first EOF a pure pulsing mode. Note that in both cases (see Fig. 6b and Fig. 7b) the first EOF of the streamfunction is dipolar, with a node somewhat poleward of the mean position of the jet and the lower band more or less coincident with the mean position of the jet. These structures are apparent in both the EOF of the zonally averaged fields, and in the zonally averaged EOF of the two dimensional fields (not shown). In the former case the variance accounted for by the first two EOFs is typically over 30% each and these are both well separated from the other EOFs. Similar structures are seen in the observations (Feldstein and Lee 1998; Lorenz and Hartmann 2001) and in simulations with a general circulation model (Cash et al. 2002). Indeed Feldstein and Lee (1998) characterize the EOFs of the northern and southern hemispheres as being either a strengthening and weakening of the jet, or a latitudinal movement of the jet, although the interpretation is complicated by additional variations in the subtropical jet.

Although useful as descriptive phrases, the pulsing and wobbling modes are not wholly independent. Recall that the mean wind was somewhat poleward of the center of the stirring, because of predominantly equatorward breaking of the Rossby waves. If the stirring is stronger, the jet is not only stronger but is pushed polewards, and the pulse and the wobble are synchronized. The EOFs are describing this in the most economical way possible, subject to their orthogonality.

c. Two-dimensional patterns

When one looks at the EOF of the two-dimensional fields, the zonal average of the first EOF (of either ve-

locity or streamfunction) is usually very similar to the EOF of the zonally average field, although the subsequent EOFs are less distinct. The first EOF normally is well separated from the others, although the variance accounted for is typically less than 20%. The first EOF of the two-dimensional streamfunction is illustrated in Fig. 8. It is nearly zonally symmetric and may be taken as a definition of the annular mode of this model. Any zonal asymmetry here can be ascribed to sampling issues, that is, a finite length of numerical integration. However, although the leading EOF is not guaranteed to be zonally symmetric, its existence should not lead one to necessarily conclude that there is a strong mode of hemispheric-wide variability in the model. The EOF analysis is again merely seeking the most economical description of model variability. In particular, in most of the integrations we have examined the zonal flow does not vary synchronously across the hemisphere. The one-point correlation function shows this quantitatively (Fig. 9). In the meridional direction, the dipolar structure of the EOF can be seen in the correlation function, especially the one centered at the pole. The zonal scale of the correlation is related to the scale of the energy containing eddies, as one might expect given that the spatial correlation function is essentially the Fourier transform of the variance of that variable (so the velocity correlation function is the Fourier transform of the energy spectrum). Thus, large-scale hemispheric-wide correlations are associated with variance in the $m = 0$ mode and, even though zonal jets are naturally produced by eddies on the sphere or β-plane, the covariability of flow around a circle of latitude may be relatively weak. Ultimately, the importance of an annular mode is related to how much eddy energy is in the zonal modes, and this is a quantitative issue that can ultimately be settled only by an appeal to observations. The spatial structure of these correlations are in fact very similar to those found in various simulations with a general circulation model (Cash et al. 2002). There too the dipole structure of the EOF is apparent, but there is little hemispheric-wide correlation.

We can obtain another sense of the hemispheric vs local nature of the variability by constructing the EOFs from a quadrant (i.e., regions 90° wide) rather than the full hemisphere. In both cases the fields are put through a 10-day running average before computing the EOFs, and these are illustrated in Fig. 10. The first EOF of the regional field is almost coincident with that constructed from the full hemispheric field, consistent with the notion that it is the same mechanism producing the variations in the zonal velocity on a hemispheric and on a regional scale. However, these variations are not always in concert. To quantify this, we compute the correlations between the daily timeseries of the principal components (PCs) corresponding to the regional and hemispheric EOFs, and between two opposing quadrants (c.f., Cohen and Saito 2002). The values of these are:

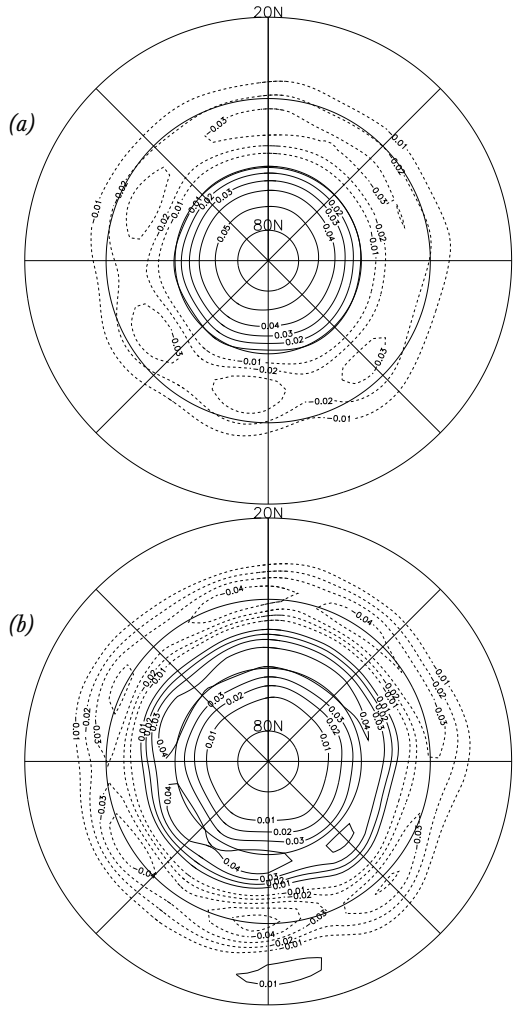

FIGURE 8: (a) The leading EOF of the streamfunction when the model is forced in a zonally symmetric configuration (Z1). (b) Leading EOF of the zonal wind. The zero contours are omitted.

$$C(Z,Q1) = 0.62 \tag{4.1a}$$
$$C(Z,Q2) = 0.63 \tag{4.1b}$$
$$C(Q1,Q2) = 0.16. \tag{4.1c}$$

Here $C(Z,Q1)$ is the temporal correlation between the PCs of the first EOF from the zonally averaged

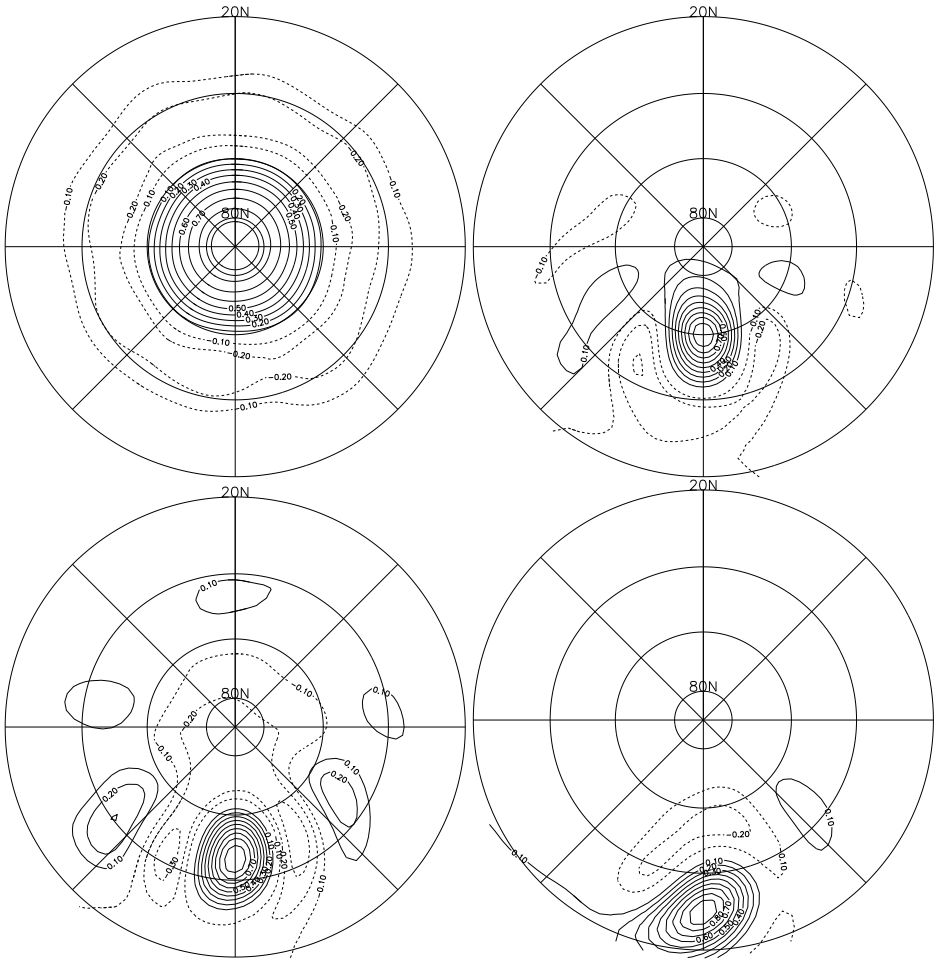

FIGURE 9: The one-point auto-correlation of the streamfunction for the same integration as Fig. 8, for four different base points (which can be identified as the points where the correlation is one). Because the statistics are zonally symmetric, the longitude of the base points is unimportant. The zero contours are omitted.

flow and that of flow in a quadrant (and similarly for $C(Z,Q2)$), and $C(Q1,Q2)$ is the correlation between the flow in the two quadrants. The difference between $C(Z,Q1)$ and $C(Z,Q2)$ is solely due to the finite length of the timeseries, and so is a measure of the error due to that.

If there were a pure annular mode in the sense that the zonal velocity varied in unison on a hemispheric scale the correlations would all be unity. If the quadrants were completely independent we would have

$$C(Z,Q1) = 0.5 \tag{4.2a}$$
$$C(Z,Q2) = 0.5 \tag{4.2b}$$
$$C(Q1,Q2) = 0. \tag{4.2c}$$

Clearly the flow here is something in between these extremes. One may conclude that although similar dynamics is acting on both the regional and hemispheric scale (because the meridional structure of the respective EOFs are so similar) this dynamics does not necessarily act in unison. We cannot expect the real atmosphere to have quantitatively the same values as (4.1), but the qualitative picture is likely to be similar.

d. Low and high index states

As noted, the mean position of the jet is slightly poleward of the center of the stirring. The stronger the jet the more poleward the mean jet position, as indicated in Fig. 11, although the effect is rather weak and the displacement of the jet is no more than 5°. However, a stronger jet is also noticeably narrower than a weak one, and the easterlies on its equatorial flank are no-

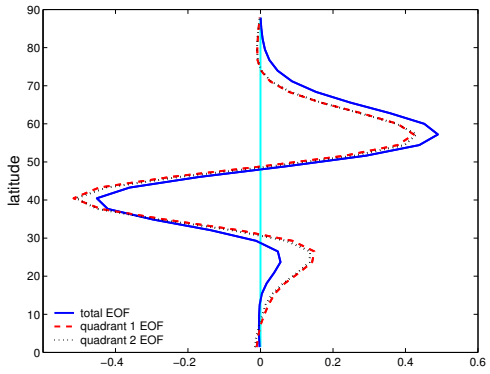

FIGURE 10: The EOF calculated from the zonally averaged flow (solid line) and from the averaged flow in two quadrants (dashed and dotted lines), for Z1.

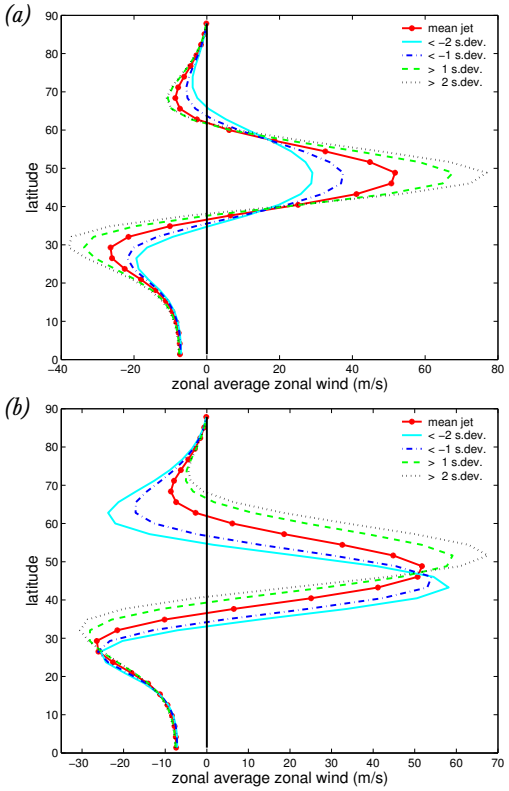

FIGURE 11: (a) Composites of the zonal wind, averaged over periods when it is particularly strong or particularly weak, for experiment Z1. The mean jet is solid, the other lines corresponding to averages over periods when its peak value deviates by more than one or two standard deviations from the mean, as indicated in the legend. (b) Composite of the zonal wind, as in (a), except now the composites are averaged over periods when the first EOF exceeds or is less than one or two standard deviations from its mean.

ticeably stronger and extend further poleward. In a model with a baroclinic subtropical jet, or the real atmosphere, the effect of this would be to enhance the separation between the eddy driven jet and the subtropical jet, and to make the midlatitude surface westerlies both stronger and slightly more poleward. Both of these effects are seen in the observations during high index states (Ambaum et al. 2001).

5. Zonally asymmetric model

a. One enhanced stirring region - the NAO

Suppose we now enhance the stirring in a longitudinal region in order to roughly mimic the effects of a storm track. However, we keep the simple meridional structure used in the zonally symmetric case, and the stirring maximum is at the same latitude for all longitudes. Specifically, the longitudinal structure of the amplitude of the stirring is

$$|F_\zeta| = A\left(1 + B\exp(-(x - x_0)^2/2\sigma^2)\right) \qquad (5.1)$$

where A and B are constants. A determines the strength of the uniform background stirring and B that of the zonal inhomogeneity, centered around longitude x_0. We have conducted experiments with B ranging from 0 to about 10, with a value of order unity best representing the enhanced stirring of the stormtrack regions over the Atlantic and Pacific. The parameter σ determines the width of the enhanced stirring region.

Fig. 12 shows the fields of eddy kinetic energy and the first EOF in an integration with $B = 1$ and an enhanced stirring region of about 45° wide, roughly comparable to the North Atlantic stormtrack. (This experiment is denoted A1; see table 1.) The eddy kinetic energy is a direct reflection of the enhanced stirring and, clearly, the EOF is centered around the enhanced stirring and reflects the more vigorous activity in that region. The localized dipole structure of the streamfunction is very similar to that appearing in zonally asymmetric GCMs (e.g., Cash et al. 2002) and in the observations (e.g., Ambaum et al. 2001). The one point correlation function (Fig. 13), with a basepoint at the longitude where the EOF is a maximum picks up the meridional dipole structure of the EOF, just as in the zonally symmetric case. In the zonal direction, the correlation function is somewhat more localized than the EOF and is not, in fact, very dissimilar from that in the zonally symmetric case Fig. 9. The day-to-day synoptic activity in the two cases is rather similar, but in the zonally asymmetric

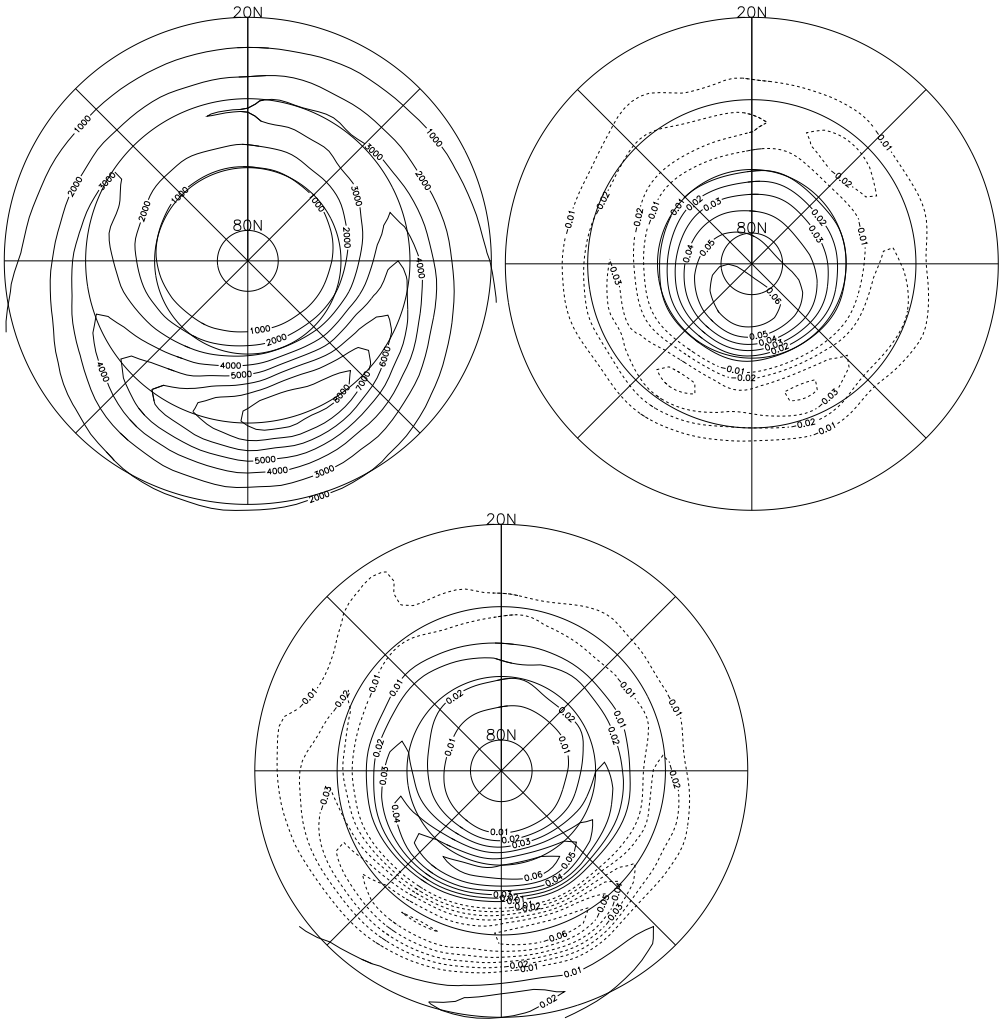

FIGURE 12: (a) Eddy kinetic energy when the model is forced in a zonally asymmetric configuration, A1, with a single enhanced region of forcing. (b) The leading EOF of the streamfunction. (c) The leading EOF of the zonal wind. The zeros contour are omitted.

case there is a slight preference for dipole structures to form in the region of enhanced stirring, and this is detected by the EOF analysis. In the zonally symmetric case, similar two-dimensional structures form locally, but with no longitudinal preference and as a consequence the first EOF is almost zonally uniform.

We also calculated the EOFs based solely on the fields in the region on the enhanced stirring, as well as the EOFs in the opposite quadrant. The EOFs in the enhanced stirring region show a similar dipole structure to those of Fig. 12 and, in an analogous fashion to (4.1), we calculate

$$C(Z,Q1) = 0.55 \tag{5.2a}$$

$$C(Z,Q2) = 0.71 \tag{5.2b}$$

$$C(Q1,Q2) = 0.11 \tag{5.2c}$$

where $Q2$ denotes the region of enhanced stirring, $Q1$ the opposite quadrant, and $C(Z,Q1)$ and $C(Z,Q2)$ are the correlations between the principal components of the zonal EOF and the regional EOFs, and $C(Q1,Q2)$ is the correlation between the two regional EOFs. Thus, the principal component of EOF constructed from the hemispheric flow has correlates well with the principal component of the EOF constructed in the region of enhanced stirring.

The structural similarity between the EOF and

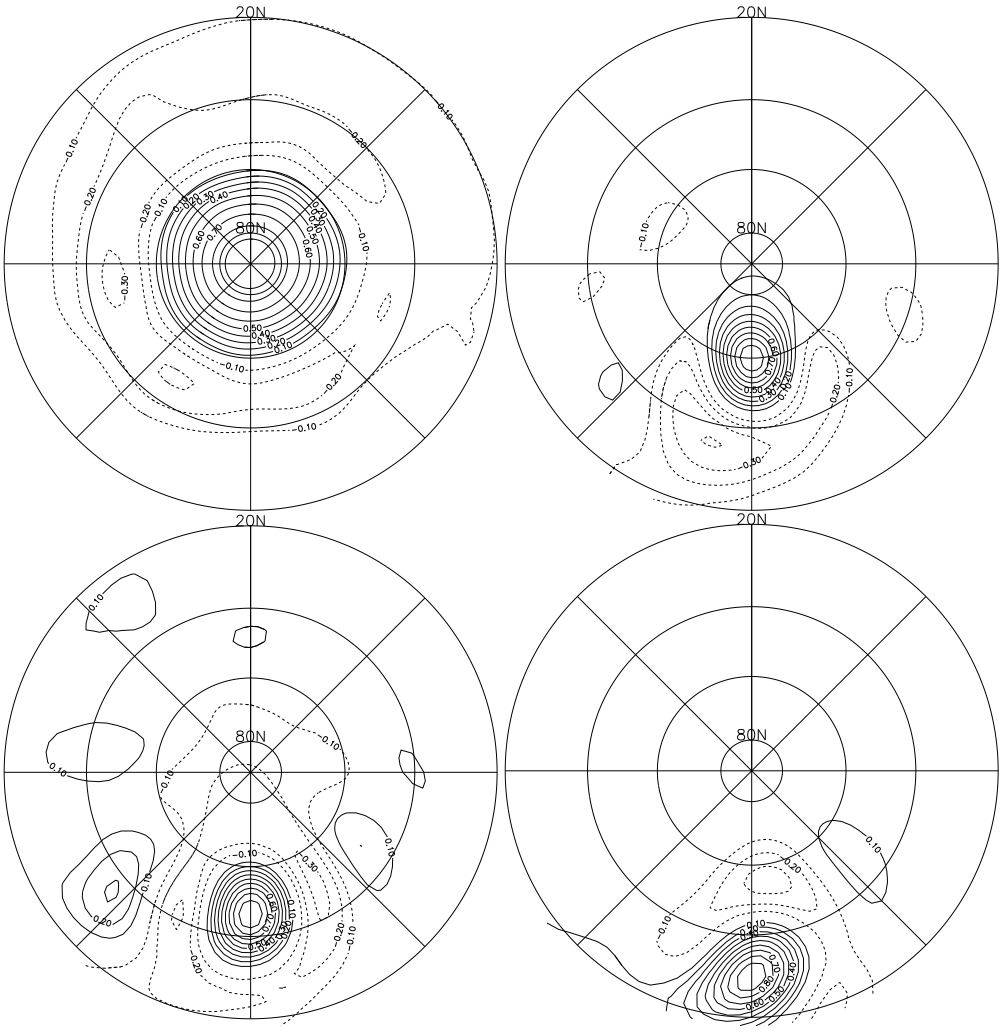

FIGURE 13: The one-point correlation of the streamfunction, for the same integration as Fig. 12, with one enhanced stirring region. The longitude of the base points is chosen to be along that of the strongest stirring, which is close to the longitude where the EOF has its maximum value. The zero contours are omitted.

the teleconnection, and the similarity between the barotropic model, the GCM results of Cash et al. (2002), and the observations, are all suggestive of the robustness of the mechanism identified. We make two additional points. First, this is a nonlinear effect. If localized stirring is added to the linear barotropic vorticity equation, then the response is a superposition of beta plumes that trail westward from the source but which produce no vorticity flux, an effect familiar to most physical oceanographers. (OF course, one might construct a linear model to mimic the nonlinear effects, but one would have to specify the structure of the vorticity fluxes.) Second, the dipole structure that is so reminiscent of the NAO arises robustly when the stirring is somewhat stronger than the zonal mean stirring (i.e., when B in (5.1) is of order one). However, if the localized stirring is extremely intense then more exotic patterns (not shown) occur. Now the theory of section 2(a) becomes invalid because of the extreme zonal inhomogeneity.

b. Two stirring regions

The Northern hemisphere has two major storm tracks, one over the Pacific and the other over the Atlantic. We model this with two stirring regions, uncorrelated from each other, and chosen to give an eddy kinetic energy pattern that roughly corresponds to that observed. The eddy kinetic energy and the

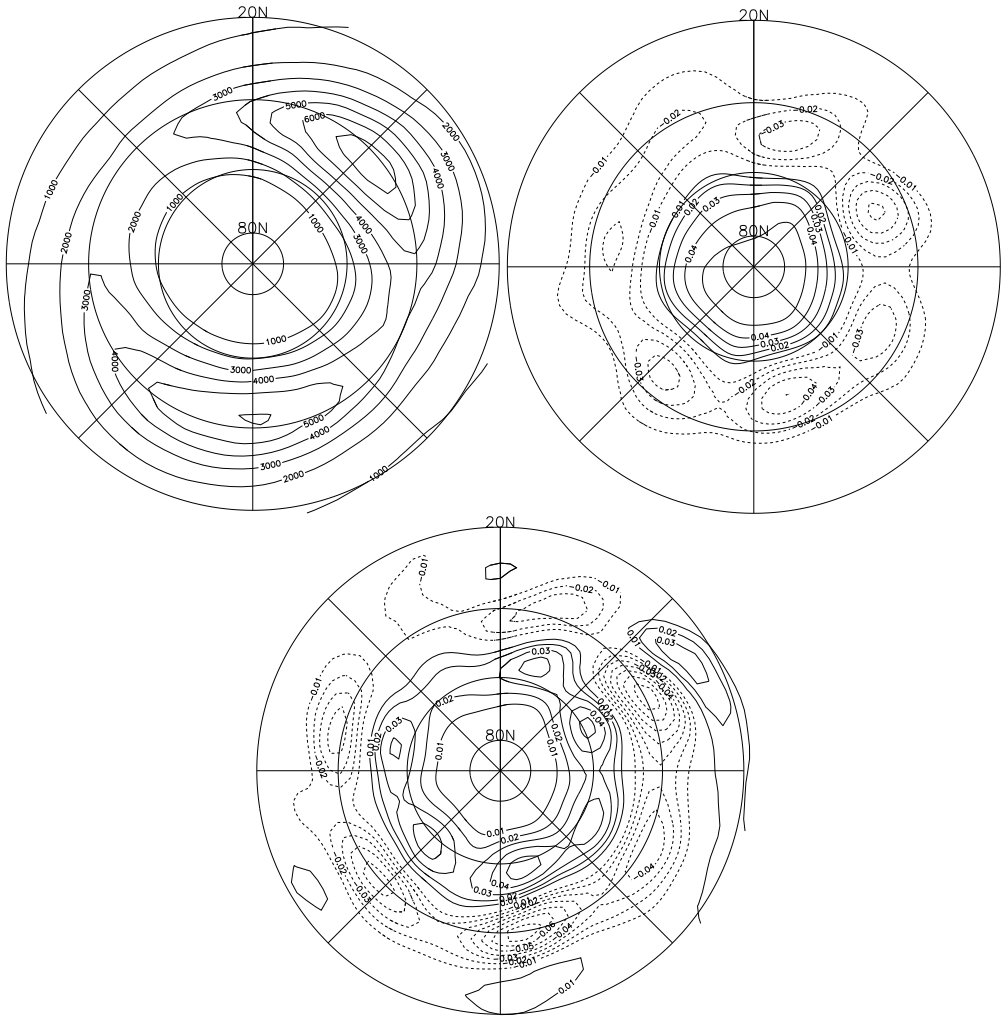

FIGURE 14: (a) Eddy kinetic energy when the model is forced in a zonally asymmetric configuration, A2, with two enhanced regions of forcing, roughly corresponding to the locations of the Atlantic and Pacific storm tracks. (b) Leading EOF of the streamfunction. (c) Leading EOF of zonal wind. The zero contours are omitted.

first EOF of streamfunction are illustrated in Fig. 14. The first EOF of the hemispheric field is quite annular, with two weak centers near the stirring regions. The one point correlation functions at these centers of action are rather similar to the case with only one storm track. The correlations between the two centers (not shown) are rather weak, increasing with the latitude of the basepoint, and there is no pronounced teleconnection between the two stirring regions.

6. Temporal Structure

Apart from the signals due to El Niño and the seasonal cycle, the large-scale patterns of extratropical variability in the atmosphere appear to have a fairly red spectrum, with no really significant peaks (Feldstein 2000). However, it is unclear whether the power in these patterns continues to increase for timescales longer than the interannual – that is, whether the spectrum continues to redden for increasingly long timescales or whether it flattens out and whitens (see Stephenson et al. 2000). Notwithstanding that uncertainty, the decorrelation timescale associated with the NAO and similar patterns is of order 10 days. Now, in our numerical model the various possible timescales are the timescale of the forcing, a frictional timescale determined by the value of r in (3.1), a nonlinear eddy turnover time for some scale L given by $L/|U_L|$ where U_L is the velocity magnitude at the scale L, and a timescale associated with Rossby wave

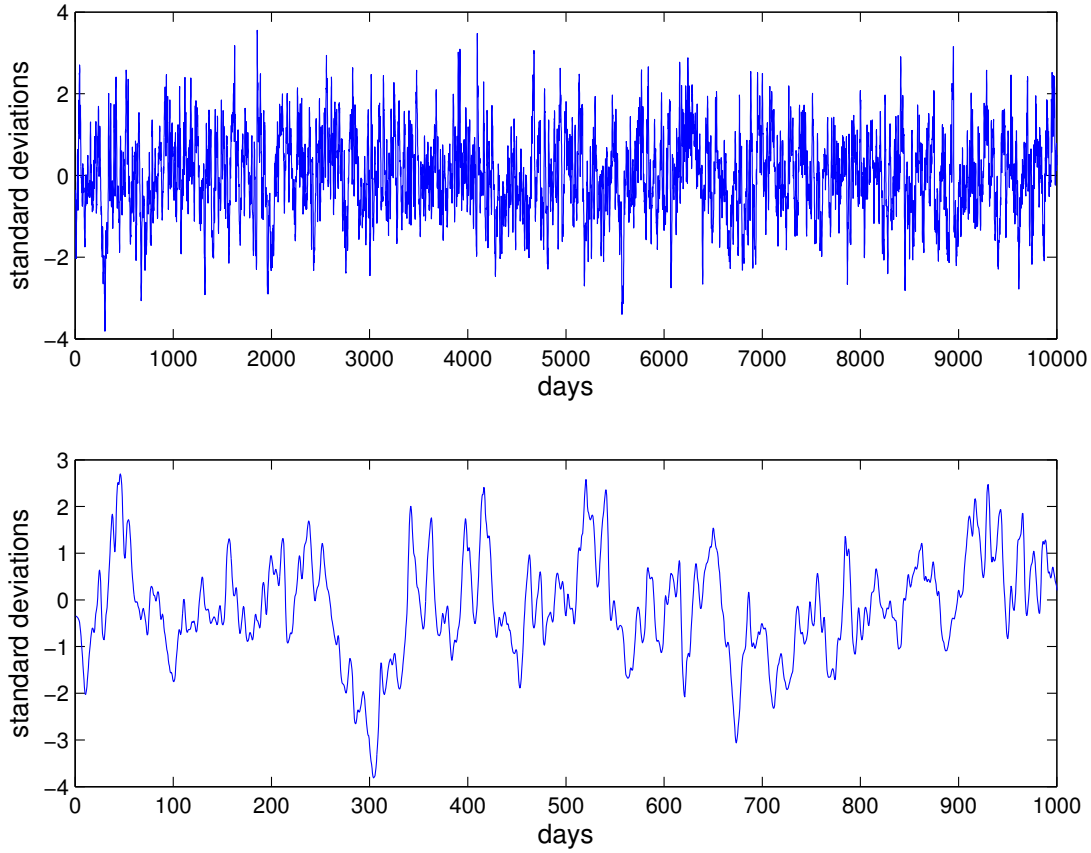

FIGURE 15: Sample timeseries of the principal component of the leading EOF of streamfunction in the zonally averaged model, Z1. The lower panel is a blow up of the first 1000 days of the upper panel.

propagation $\sim 1/(L\beta)$. The external parameters are those associated with the forcing and friction – the eddy turnover time is ultimately given by the magnitude of the forcing and how effective it is in generating flow. If we choose our forcing decorrelation time to be of order a few days to represent baroclinic activity, then we must tune its magnitude to give flow velocities with a magnitude similar to those observed, and in that case the only remaining external free parameters are r and β.

Friction is clearly an important element in the reddening of the forcing spectrum, as we see from the linear version of (3.1). The equation is

$$\frac{\partial \zeta}{\partial t} + \beta \frac{\partial \psi}{\partial x} = S - r\zeta \tag{6.1}$$

and this can be solved analytically if the power spectrum of S is known, assuming a solution of the form

$$\psi = Re\Psi e^{i(\mathbf{k}\cdot\boldsymbol{x}-\omega t)}. \tag{6.2}$$

Substituting into (6.1) gives

$$|\Psi|^2 = \frac{S_\omega^2}{[(k^2\omega + \beta k_x)^2 + r^2 k^4]} \tag{6.3}$$

and so the forcing spectrum is reddened. The solution is completed by the addition of the homogeneous problem, a decaying Rossby wave.

Numerical solutions of the nonlinear problem show this effect – in Fig. 15 we see a representative timeseries of the first EOF in a zonally symmetric simulation. (The EOF itself is first obtained using temporally low-passed data, but the figure shows the daily, unfiltered, values of the corresponding principal component.) Fig. 16 show the corresponding power spectra, which are characteristically red, with more power at low frequencies when the friction is small. The auto-correlation of the first two EOFs is shown in Fig. 17, and these are of order 10 days. The wobbling mode typically has a longer decorrelation than the pulse, but as noted previously these two modes are not wholly independent and as the

jet wobbles from one extreme latitude to another it passes through its mean location twice. For shorter timescales the decorrelation timescale (the e-folding timescale) is approximately equal to the frictional timescale, as expected in an Ornstein-Uhlenbeck type process. However, inspection of Fig. 16a and Fig. 17b indicates that the correlation timescale does not increase as quickly as the frictional timescale increases; for frictional timescales of 12 days, 23 days and 43 days we find decorrelation timescales of 10 days, 15 days and 19 days respectively, in a 300 year simulation. Evidently, the chaotic dynamics of the large-scale fields are limiting the temporal correlations. Somewhat unexpectedly, the auto-correlation of the simulation with the higher damping (12 days) has a shoulder at about 40 days, and has virtually as much power at very long times as the simulation with a 23-day damping timescale, anothe indication that frictional effects are not the sole determinant of the power at low-frequencies. (The correlation and power spectra are quite robust, coming from a 300 year simulation.) Note that it is also apparent from the timeseries that quite long excursions from the mean are possible. For example, there is almost a 500 day excursion between 6000 and 7000 days, and frequent excursions of order 100 days – note for example the dip centered around 300 days. [Long term variability was also found by James and James (1992) in a simplified general circulation model, although the variability they found involved the subtropical jet, which is absent in this model.]

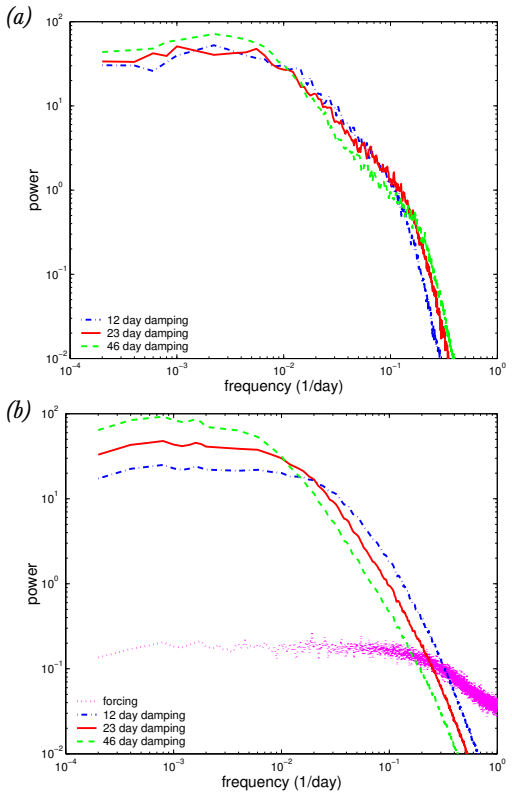

FIGURE 16: (a) Power spectra of the principal components of the leading EOFs of the streamfunction in zonally symmetric integrations with varying values of the frictional parameter r, corresponding to frictional timescales of approximately 12 days, 23 days and 46 days, with forcing as in Z1. (b) Power spectral of the stochastic process, $dz/dt = S - rz$, for the same three values of r used in (a), and S, the stochastic forcing, also having the same power spectra as used to force the model. The timeseries are normalized to have the same variance.

7. Summary and Conclusions

We have presented a simple dynamical model of the North Atlantic Oscillation and the related annular modes. We have shown that spatial structures similar to those associated with the North Atlantic Oscillation and annular modes can be robustly and easily reproduced with a stochastically forced, but nonlinear, nondivergent barotropic model. The stochastic forcing has a very simple spatial structure and need not be extensively tuned for the patterns to appear.

The model suggests that the NAO and annular modes are, essentially, two sides of the same coin. The (single) phenomenon is associated with variations in the midlatitude circulation caused by fluctuating stirring from baroclinic eddies. The fluctuating stirring produces both a variation in the intensity and position of the zonal jet, and a dipolar circulation anomaly. This in turn leads to a dipolar structure in the streamfunction (i.e. the pressure field) variability, and so a dipolar EOF, much as is observed.

If the eddy statistics are zonally uniform, then the leading EOF of the zonal velocity and the streamfunction are also zonally uniform. Wave-meanflow interaction has produced variability in the zonally averaged flow, and this may be interpreted or defined as an annular mode. However, the variability of an annular mode is (in this interpretation) not the hemispheric-wide synchronous variability or heaving of a polar vortex. Rather, it is the projection onto the zonally averaged flow of eddy dynamics.

The North Atlantic Oscillation is to be differentiated from the annular mode primarily by its scale, not its mechanism. The presence of an Atlantic stormtrack provides stronger stirring, and if the longitudinal extent of the stormtrack is greater than that of a single eddy, the same dynamics that produce varia-

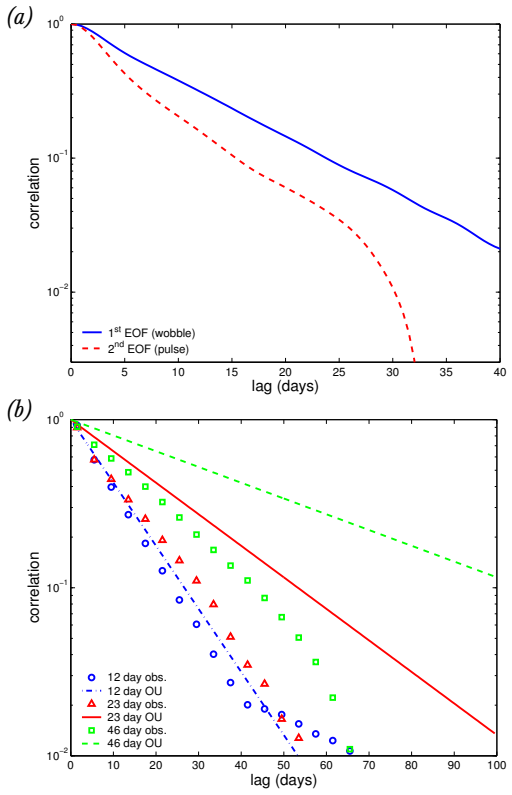

FIGURE 17: (a) Autocorrelation of the principal components (PCs) of the first two EOFs of a zonally symmetric integration (Z1), with a frictional timescale of 12 days. (b) Autocorrelations of the PCs of the first EOFs of three model integrations, each with a different value of the damping timescale (denoted 'obs'), and the autocorrelations for three Ornstein-Uhlenbeck processes with the same damping timescales (denoted OU).

.

tions of the zonally averaged flow will still act, just more intensely, over that region. Thus, the jet variations will be stronger here than elsewhere, and any measure of that variability, such as the first EOF of pressure or streamfunction, will show a dipole centered near the eddy activity. Now, when the stirring is stronger – i.e., when the stormtrack is stronger – the barotropic jet is strengthened and tightened, whereas any subtropical jet would be little altered. Thus, during periods of high eddy activity the eastward advection will be strongest at latitudes poleward of its mean position. Conversely, quiescent periods will have a weaker barotropic jet and the eastward advection will be somewhat equatorward of its mean position. Thus, at one extreme we can expect eddy-rich activity with a strong eastward jet somewhat poleward of its mean position; at the other extreme we expect weaker eddy activity with a weaker, slightly more equatorward jet. This is, of course, the manifestation of the NAO.

Another way of expressing this is to say that it is the organization of the baroclinic activity into spatially coherent large scale patterns (i.e., storm tracks) that gives rise to coherent large scale vorticity stirring, and this in turn produces patterns like the NAO. Because the mean amplitude of the vorticity-stirring varies zonally, the eddy forcing has a stationary component (i.e., there is a zonal asymmetry in the time mean eddy fluxes) and it is this stationary component that produces the NAO. Momentum fluxes from stationary waves are really the same as the spatially nonuniform eddy fluxes we have parameterized, and that such forcing is responsible for the zonally asymmetric patterns of variability seems consistent with the observational analyses of Limpasuvan and Hartmann (2000).

If this mechanism is the case, then there should be a corresponding phenomena in the Pacific as well as the Atlantic corresponding to the Pacific stormtrack. Such a 'North Pacific Oscillation' may well exist [indeed Walker and Bliss (1932) commented on it] although it may not be as noticeable as the NAO both because the high frequency variability in the Pacific is less than in the Atlantic, and because there are many other phenomena occurring in the Pacific, such as ENSO, the Pacific North American pattern and the Pacific Decadal Oscillation. There may well be additional, more subtle differences in the stormtracks between these regions and we recognize that the differences between the NAO and NPO are unlikely to be fully explained by our proposed mechanism. [A potentially related issue is that there seems to be an observed tendency for the maximum amplitude of the EOFs to be located a little downstream of the storm tracks. We might expect this because momentum fluxes occur primarily in the decaying phase of the baroclinic lifecycle, and thus downstream of the center of the stormtracks. Such a mechanism cannot be reproduced in a barotropic model, but nor, in fact, is it a robust feature of simulations with GCMs (Cash et al. 2002).]

The decorrelation timescale of the NAO and annular modes are observed to be about 10 days, and this is well reproduced by the model, albeit it is partly dependent on the frictional timescale chosen. The eddy forcing itself, even the stationary-eddy forcing, has a much shorter decorrelation timescale (a day or two) and this is reddened by damping processes and, to some degree, nonlinear dynamics. The barotropic model does produce variability on long timescales,

evidently up to 1000 days, although the presence of a seasonal cycle might affect this. Determining whether this long-term variability corresponds to that seen in the observations will require a more detailed study of both model and observations, since the nature of such long-term variability is currently unclear in both. [Feldstein (2000) concludes that the NAO is a Markov process with an e-folding timescale of about 10 days, whereas Stephenson et al. (2000) note the presence of 'long-range dependencies' (a red spectrum) on interannual timescales. These may not be contradictory, if the tails in the autocorrelations are nonzero but small.]

What is particularly notable about the model we have presented is what is *not* in it – for example, there is neither a stratosphere nor an ocean. While these and other factors may, of course, contribute to the persistence and intensity of the NAO and annular modes, our results show that neither of them is necessary for the basic existence or the spatial structure of these patterns. The model does suggest that the ocean might influence the interannual variability of the NAO by affecting baroclinic activity and the stormtrack, but has less to say concerning stratospheric influences on the structures. Another simplification in this model is that baroclinic effects are modeled by a simple wavemaker that is not related to the strength of the barotropic jet (although the ensuing pseudomomentum stirring is organized by the jet structure). This suggests that a state dependence of the stirring is not a crucial ingredient of annular mode or NAO structure. If we were to construct a model in which the stirring were to depend on the strength of the jet, the eddies might then follow the position of the jet and a longer timescale might thereby be produced – but this is a speculative comment. Careful studies with both parameterized models and a trustworthy GCM may be needed before one can definitively determine the importance of such a feedback mechanism between eddies and zonal flow in producing intraseasonal variability, especially as the observations do not clearly discount a simpler stochastic process. Finally, we point out that the dynamics of the variability of a stochastically forced jet have not been fully elucidated.

To conclude, we have presented a simple, dynamically robust mechanism that reproduces some of the important spatial and temporal characteristics of the large-scale variability in the atmosphere. We hope it may be useful as a dynamical basis for more complete models and simulations, and in interpreting the observations.

Appendix

Consider the Ornstein-Uhlenbeck process S given by the stochastic differential equation

$$\frac{dS}{dt} = -\frac{S}{\tau} + \frac{\sigma\sqrt{2}}{\sqrt{\tau}}\dot{W} \tag{A.1}$$

with $S(0) = S_0$. Suppose that S_0 is chosen from some initial distribution, to be determined below. S is a Gaussian process, and thus wholly characterized by its mean and covariance functions,

$$E[S(t)] = e^{-t/\tau}E[S_0] \tag{A.2}$$

$$\mathrm{cov}(S(s), S(t)) = e^{-(s+t)/\tau}\mathrm{var}(S_0) + \sigma^2 e^{-(t-s)/\tau} - \sigma^2 e^{-(s+t)/\tau} \tag{A.3}$$

where $s \le t$. When $s, t >> 0$, the mean and covariance functions approach

$$E[S(t)] \to 0 \tag{A.4}$$

$$\mathrm{cov}(S(s), S(t)) \to \sigma^2 e^{-(t-s)/\tau} \tag{A.5}$$

regardless of the initial distribution of S_0. In our model we are interested in the long term statistical behavior of the system and so lose nothing by taking the initial distribution of S_0 to be the asymptotic distribution, $N(0, \sigma^2)$. In this case, (A.2) and (A.3) become (A.4) and (A.5).

We can then simulate $S(t)$ with the finite difference equation

$$S^i = \sqrt{1 - e^{-2dt/\tau}}\,\phi^i + e^{-dt/\tau}S^{i-1} \tag{A.6}$$

where dt is our time step and the ϕ^i and S^0 are random variables taken from the Guasian distribution $N(0, \sigma^2)$. The paths $S^0, S^1, S^2, \ldots$ are equivalent to paths of $S(t)$ sampled at increments of dt. This follows from the fact that $\{S^i\}$, as a series of sums of Guassian variables, is a Guassian process, and thus characterized by its mean and covariance

$$E[S^i] = 0 \tag{A.7}$$

$$\mathrm{cov}(S^i, S^j) = \sigma^2 e^{-(j-i)dt/\tau} \tag{A.8}$$

for $i \le j$, which match the properties of the continuous process above. In our implementation of (A.6), we sample the ϕ^i from a uniform distribution centered about zero, rather than a Gaussian. The modified process is not precisely an Ornstein-Uhlenbeck process: it has the same mean and covariance structure of S, but slightly different higher moments. It proved advantageous in avoiding occasional large (and unrealistic) spikes in a single wavenumber.

References

Ambaum, M. H. P., B. J. Hoskins, and D. B. Stephenson, 2001: Arctic Oscillation or North Atlantic Oscillation? *J. Climate*, **14**, 3495–3507.

Branstator, G., 1992: The maintenance of low-frequency anomalies. *J. Atmos. Sci.*, **49**, 1924–1945.

Cash, B. A., P. Kushner, and G. K. Vallis, 2002: Zonal asymmetries, teleconnections, and annular models in a GCM. *J. Atmos. Sci.*, (submitted).

Cohen, J., and K. Saito, 2002: A test of annular modes. *J. Climate*, **15**, 2537–2546.

DeWeaver, E., and S. Nigam, 2000: Zonal-eddy dynamics of the North Atlantic Oscillation. *J. Climate*, **13**, 3893–3914.

Feldstein, S. B., 2000: The timescale, power spectra and climate noise properties of teleconnection patterns. *J. Climate*, **13**, 4430–4440.

Feldstein, S. B., and S. Lee, 1998: Is the atmospheric zonal index driven by an eddy feedback? *J. Atmos. Sci.*, **55**, 3077–3086.

Held, I. M., 2000: *The General Circulation of the Atmosphere*. Proc. Woods Hole Summer School on GFD, 66 pp.

James, I., and P. M. James, 1992: Spatial structure of ultra-lowfrequency variability of the flow n a simple atmospheric circulation model. *Quart. J. Roy. Meteor. Soc.*, **118**, 1211–1233.

Lau, N.-C., 1988: Variability of the observed midlatitude storm tracks in relation to low-frequency changes in the circulation pattern. *J. Atmos. Sci.*, **45**, 2718–2743.

Lee, S., 1997: Maintenance of multiple jets in a baroclinic flow. *J. Atmos. Sci.*, **54**, 1726–1738.

Limpasuvan, V., and D. L. Hartmann, 2000: Wave-maintained annular modes of climate variability. *J. Climate*, **13**, 4414–4429.

Lorenz, D. J., and D. L. Hartmann, 2001: Eddy-zonal flow feedback in the Southern Hemisphere. *J. Atmos. Sci.*, **58**, xxx.

Maltrud, M. E., and G. K. Vallis, 1991: Energy spectra and coherent structures in forced two-dimensional and beta-plane turbulence. *J. Fluid Mech.*, **228**, 321–342.

Orlanski, I., 1998: On the poleward deflection of storm tracks. *J. Atmos. Sci.*, **55**, 128–154.

Rhines, P. B., 1977: The dynamics of unsteady currents. E. A. Goldberg, I. N. McCane, J. J. O'Brien, and J. H. Steele, Eds., *The Sea*, Vol. 6, J. Wiley and Sons, 189–318.

Robinson, W. A., 2000: A baroclinic mechanism for eddy feedback on the zonal index. *J. Atmos. Sci.*, **57**, 415–422.

Salmon, R., 1980: Baroclinic instability and geostrophic turbulence. *Geophys. Astrophys. Fluid Dyn.*, **10**, 25–52.

Simmons, A., and B. Hoskins, 1978: The life-cycles of some nonlinear baroclinic waves. *J. Atmos. Sci.*, **35**, 414–432.

Smith, K. S., G. Boccaletti, C. Henning, I. Marinov, F. Tam, I. Hed, and G. K. Vallis, 2002: Turbulent diffusion in the geostrophic inverse cascade. *J. Fluid Mech.*, **77**, 34–54.

Stephenson, D. B., V. Pavan, and R. Bajariu, 2000: Is the North Atlantic Oscillation a random walk? *Int. J. Climatology*, **20**, 1–18.

Thompson, D. W. J., and J. M. Wallace, 2000: Annular modes in the extratropical circulation. Part I: Month-to-month variability. *J. Climate*, **13**, 1000–1016.

Vallis, G. K., and M. E. Maltrud, 1993: Generation of mean flows and jets on a beta plane and over topography. *J. Phys. Oceanog.*, **23**, 1346–1362.

Walker, G. T., and E. W. Bliss, 1932: World weather v. *Memoirs of the R. M. S.*, **4**, 53–83.

Wallace, J. M., 2000: North Atlantic Oscillation/Annular Mode: Two paradigms – one phenomenon. *Quart. J. Roy. Meteor. Soc.*, **126**, 791–805.

Wallace, J. M., and D. S. Gutzler, 1981: Teleconnections in the geopotential height field during the Northern Hemisphere winter. *Mon. Wea. Rev.*, **109**, 784–812.

Wanner, H., S. Bronnimann, C. Casty, D. Gyalistras, J. Luterbacher, C. Schmutz, D. B. Stephenson, and E. Zoplaki, 2002: North Atlantic Oscillation – concepts and studies. *Surveys in Geophysics*, **22**, 321–381.

Whitaker, J. S., and P. D. Sardeshmukh, 1998: A linear theory of extratropical eddy statistics. *J. Atmos. Sci.*, **55**, 237–258.